Electronic Supplementary Material (ESI) for Soft Matter.

Supplementary information for “Embedding orthogonal memories in a colloidal gel through oscillatory shear"

Eric M. Schwen,[*a] Meera Ramaswamy,[a] Chieh-Min Cheng,[b] Linda Jan,[b] and Itai Cohen[a]

[a]*Department of Physics, Cornell University, Ithaca, NY 14850, USA*

[b]*Xerox Corporation, Rochester, NY 14605, USA*

E-mail: ems445@cornell.edu

November 7, 2019

S1 Training strain extremes

Measurements of the gel response for zero training strain show that no memory is formed without shear training. To measure the gel response at $\gamma_0 = 0$, we let the gel sit without shearing for the same period of time as the normal shear training procedure. As it sits, we image the static gel at the same frequency we normally would for stroboscopic images during training. The image difference over time is plotted in Fig. S1a and shows no significant change over time. Strain amplitude sweeps taken as normal before and after this wait period and show no significant difference (Fig. S1b). No "memory" is formed in the gel and no measurable changes are observed. This check confirms that our measured memory effect does not emerge through normal gel aging.

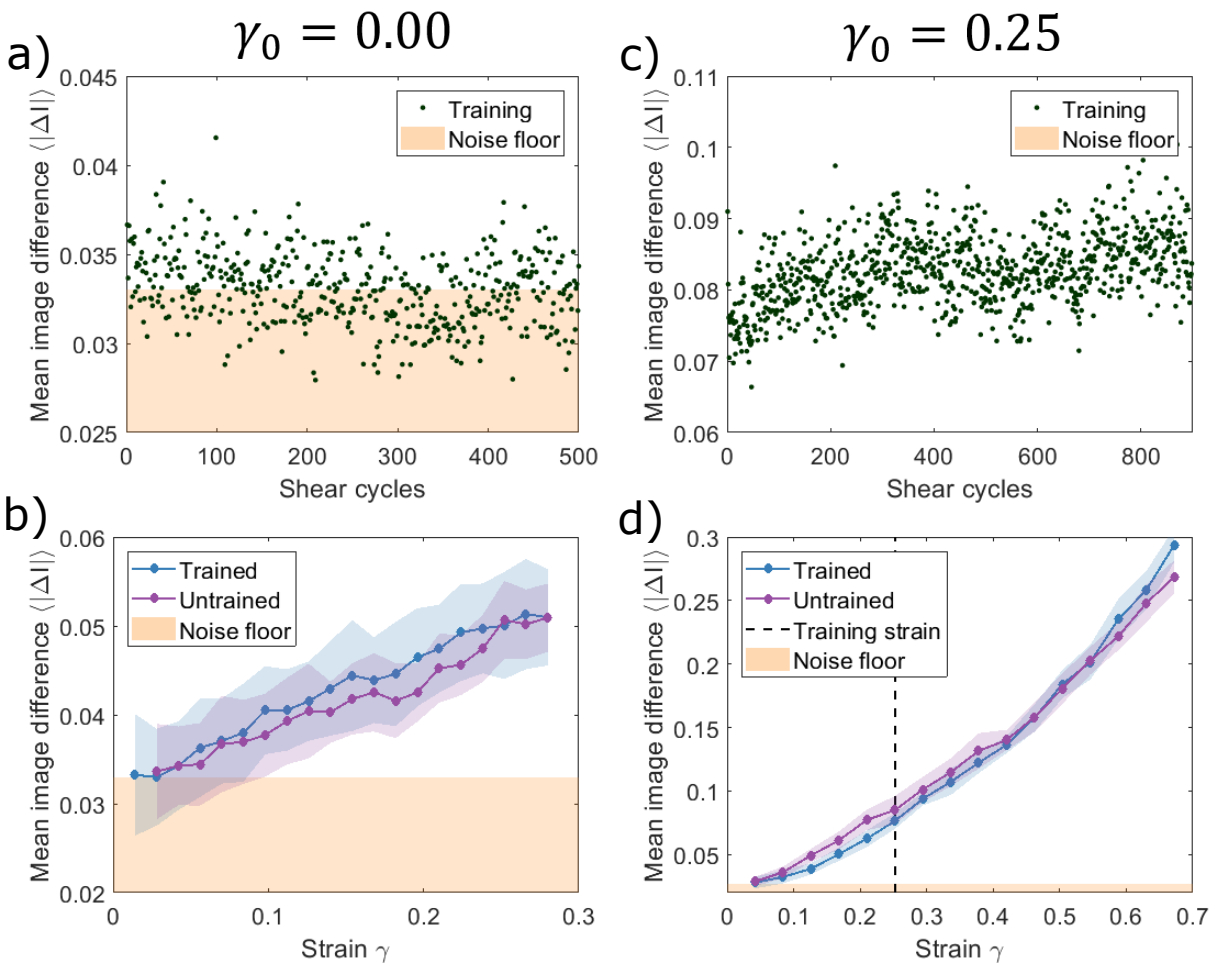

Figure S1 Mean image difference $\langle|\Delta I|\rangle$ as a function of time while waiting without shearing. X-axis shows equivalent time for "shear cycles" at 0.2 Hz following the form of similar plots. (b) Strain amplitude sweep at 0.2 Hz comparing the shear response of the gel before and after waiting. (c) Mean image difference $\langle|\Delta I|\rangle$ as a function of shear cycles for training strain $\gamma_0 = 0.25$ at frequency 0.5 Hz. (d) Strain amplitude sweep comparing the shear response of the gel from (c) before and after training.

Image difference for very high training strains show another expected result—no memory is formed if the training strain is too high for stable structures to form. The image difference over time for $\gamma_0 = 0.25$ at 0.5 Hz shows no net decrease over the training period (Fig. S1c). The gel continues the same amount of rearrangement as long as it is sheared.

The strain amplitude sweep shows no significant difference between the untrained and trained gel (Fig. S1d). This null result is expected for high enough training strains. The large strain rips apart gel structures and prevents the formation of structures that could shear without rearranging.

S2 Characteristic training time

For our gels, the mean image difference $\langle|\Delta I|\rangle$ during shear training decreases towards a steady-state value at long times. The decrease is well fitted by the form $\langle|\Delta I|\rangle = (\langle|\Delta I|\rangle_0 - \langle|\Delta I|\rangle_\infty)\exp(-t/\tau) + \langle|\Delta I|\rangle_\infty$ where $\langle|\Delta I|\rangle_0$ and $\langle|\Delta I|\rangle_\infty$ are the initial and steady-state image difference values, t is time measured in shear cycles, and τ is the characteristic time to reach steady state (see main Fig. 2). The characteristic time τ varies with training strain amplitude γ_0 and appears to diverge at a critical training strain γ_0^c. This critical training strain marks the division between reversible steady states below and steady states with rearrangement above. The characteristic time divergence is consistent with power-law scaling of the form $\tau \sim |\gamma_0 - \gamma_0^c|^{-\nu}$ similar to that seen in other memory-forming disordered systems. However, experiments to precisely measure the critical training strain γ_0^c and scaling exponent ν require long times of $\sim$ 8 hours over which we observed drift in particle properties. This time constraint limited any set of measurements to a maximum of $\sim$ 6 different training strains. Additionally, the critical strain seemed to vary between preparations. In order to compare different preparations, we fit the characteristic times for each preparation to the scaling form $\tau \sim |\gamma_0 - \gamma_0^c|^{-\nu}$ and determined the critical strain γ_0^c (Fig. S2a). We then combined the data sets from the different preparations to measure the critical exponent $\nu = 0.7 \pm 0.2$ (Fig. S2b). The limited time for trials and variation between preparations prevent easy measurement of a more precise critical exponent with this gel system.

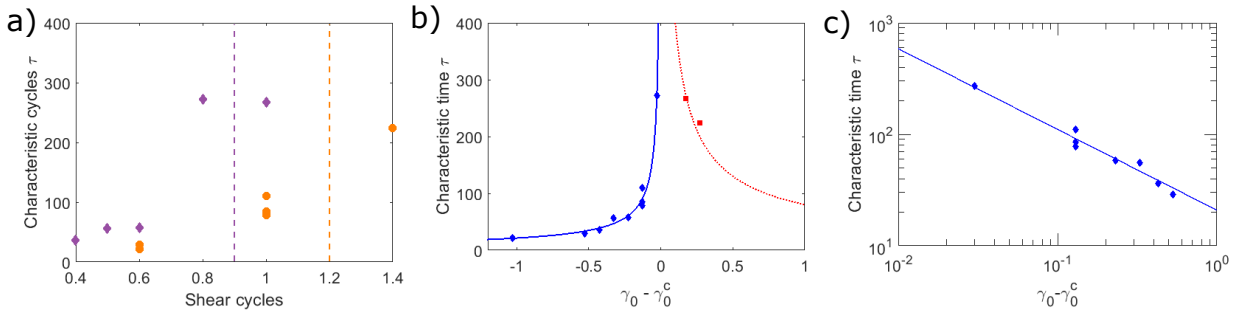

Figure S2 Characteristic training time. (a) Characteristic training time τ plotted vs. training strain γ_0 for different sample preparations at $\phi = 0.35\%$. Dotted vertical lines mark the calculated critical strain γ_0^c for each preparation. (b) Combined plot of characteristic training times τ for different sample preparations. Solid blue line shows the power-law fit $\tau \sim |\gamma_0 - \gamma_0^c|^{-\nu}$ with $\nu = 0.7 \pm 0.2$. Dotted red line sketches decreasing τ at high strains. (c) The same data for $\gamma_0 < \gamma_0^c$ plotted on a log-log scale.

S3 Voronoi volumes

An alternative method of analyzing nearest neighbors and local structure relies on Voronoi tessellation. For Voronoi tessellation, the full 3D space of the image is divided into volumes based on the distance to the gel particles. Each particle has a Voronoi volume made up of all points closer to to it than to any other particle. The magnitude of that volume can serve as a measure of the amount of free space around the particle.

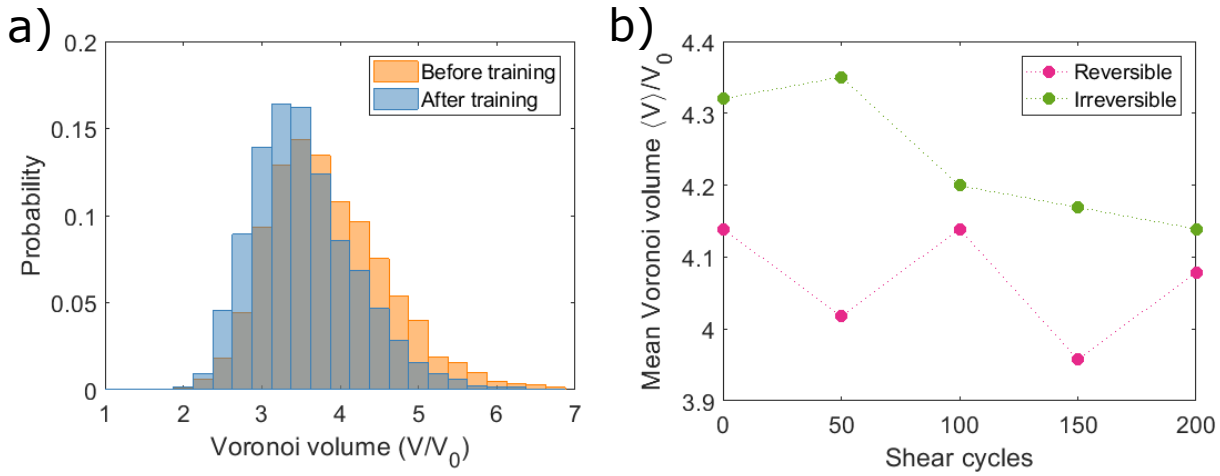

Figure S3 (a) Distribution of Voronoi volumes V before and after training scaled by single particle volume V_0. (b) Mean Voronoi volume scaled by single particle volume V_0 for reversible and irreversible particles at different points in training process. Results are shown for a $\phi = 35\%$ gel at training strain $\gamma_0 = 0.06$ at 0.33 Hz with particles located using centroid-tracking methods.

We calculate the Voronoi volumes for particles in our gel before and after shear training as well as for pauses during the training process. After training, the distribution of Voronoi volumes peaks at a lower value with a longer tail extending to high volumes. This observation suggests slight densification where the gel divides into more dense regions and larger voids (Fig. S3a). Returning to the designation of reversible and irreversible particles can give some insight into how Voronoi volume relate to particle rearrangement. We find that irreversible particles tend to have a larger Voronoi volume than reversible ones (Fig. S3b). This pattern continues during the training process and fits in with our contact number observations. Particles with many close neighbors will have small Voronoi volumes and will not rearrange. The particles with larger Voronoi volumes are more likely to be on the edges of structures and are more likely to move between cycles.

S4 Bond angles

The distribution of bond angles can show whether particles are preferentially forming chains in response to shear flow. We locate particles using centroid-based methods and then parameter extraction from reconstructing images (PERI). Using centroid-based methods, we locate all particles in 3D image stacks (64x64x6 μm) and define neighboring particles to be in contact if their center-to-center distance is less than 2.1 μm in order to account for the contact range but also allow for polydispersity and uncertainties in particle positions. A sample probability density function for bond angles of a trained gel projected into the shear-vorticity plane is shown in Fig. S4a. A preference for particles chaining along the shear flow direction would appear as a peak at 0°. We instead see an isotropic distribution of bond angles, suggesting that the reversible structures formed under training extend into the shear-vorticity plane as well. Similar results are found for particles located using PERI where we define bonds as particles with surface separations less than 50 nm (Fig. S4b). Noise is much higher due to the smaller subset of particles located, but the lack of a preferential bond direction remains.

The bond angle distribution projected into the shear-gradient plane is plotted in Fig. S4c and shows a non-isotropic structure. Particles tend not to stack directly on top of each other, as shown by the low probability of finding a bond at 0°

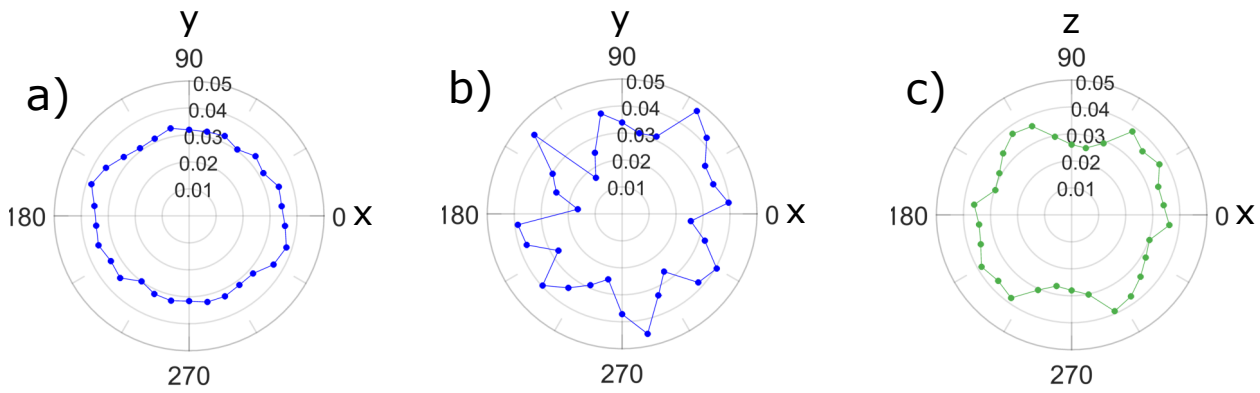

Figure S4 (a) Probability density function for gel bond angles after training projected into the shear-vorticity plane. Bond angles for this plot are determined for particles with center-to-center separation less than 2.1 μm. (b) Same probability density function as (a) but using a smaller subset of particles located precisely using PERI. Variation from isotropic distribution is within noise. (c) Probability density function for gel bond angles after training projected into the shear-gradient plane. Bond angles for this plot are determined for particles with center-to-center separation less than 2.1 μm. These data are for a gel after training with $\gamma_0 = 0.14$ at 0.33 Hz and are representative of the results we find for other parameters.

or 180°. A similar distribution shape is found both before and after training, suggesting that it is not the result of the shear training process. It may instead arise from gravitational effects or the relatively narrow gap between the top and bottom plates (15 particle diameters compared to hundreds in the other directions).